

# NJC

Accepted Manuscript



This is an *Accepted Manuscript*, which has been through the Royal Society of Chemistry peer review process and has been accepted for publication.

*Accepted Manuscripts* are published online shortly after acceptance, before technical editing, formatting and proof reading. Using this free service, authors can make their results available to the community, in citable form, before we publish the edited article. We will replace this *Accepted Manuscript* with the edited and formatted *Advance Article* as soon as it is available.

You can find more information about *Accepted Manuscripts* in the [Information for Authors](#).

Please note that technical editing may introduce minor changes to the text and/or graphics, which may alter content. The journal's standard [Terms & Conditions](#) and the [Ethical guidelines](#) still apply. In no event shall the Royal Society of Chemistry be held responsible for any errors or omissions in this *Accepted Manuscript* or any consequences arising from the use of any information it contains.



[www.rsc.org/njc](http://www.rsc.org/njc)

Cite this: DOI: 10.1039/c0xx00000x

www.rsc.org/xxxxxx

ARTICLE TYPE

## Chemical fixation of CO<sub>2</sub> into Cyclic Carbonates by azo-containing Schiff Bases metal complexes

Mesut İkiz,<sup>a</sup> Esin İspir,<sup>a\*</sup> Emine Aytar,<sup>b</sup> Şemistan Karabuğa,<sup>a</sup> Mehmet Aslantaş,<sup>c</sup> Ömer Çelik,<sup>d</sup> Mahmut Ulusoy<sup>b</sup>

Received (in XXX, XXX) Xth XXXXXXXXX 20XX, Accepted Xth XXXXXXXXX 20XX

DOI: 10.1039/b000000x

Two new ligands containing -N=N- group, 4-((E)-(4-bromophenyl)diazenyl)-2-((E)-(phenylimino)methyl)phenol (L<sup>1</sup>H **2**), 4-((E)-(4-bromophenyl)diazenyl)-2-((E)-(4-ethylphenyl)imino)methyl)phenol (L<sup>2</sup>H **3**) and their metal complexes were synthesized. The synthesized metal complexes were performed as catalysts for the chemical fixation of CO<sub>2</sub> into cyclic carbonates using epoxides which were used as both substrate and solvent. According to analytical, UV-visible and IR data, the metal complexes are formed by coordination of the N, O atoms of the ligands and metal:ligand ratio was found to 1:2 for all the complexes. TG and DTA results showed that these complexes had good thermal stability. Molecular structures of the ligand (L<sup>1</sup>H **2**) and its Zn<sup>II</sup> complex **4** (Zn(L<sup>1</sup>)<sub>2</sub>) were determined by single crystal X-ray diffraction studies. After choosing the best active catalyst (Zn(L<sup>1</sup>)<sub>2</sub>**4**), the optimization studies were performed by changing various parameters. Ionic Liquid has been found to have a positive effect and showed the best active performance with (bmim)PF<sub>6</sub><sup>+</sup> Zn(L<sup>1</sup>)<sub>2</sub>**4** as binary catalytic system.

**Keywords:** Schiff Base complexes; azo compounds, catalysts, carbon dioxide, cyclic carbonate, X-ray crystallography

### Introduction

Fossil fuels which give CO<sub>2</sub> as a by-product are the main sources of energy despite of new different energy sources such as wind, sun, geothermal *etc.*. Fossil fuel burning is the primary source of CO<sub>2</sub> emission<sup>1</sup>. CO<sub>2</sub> is a renewable source of carbon and identified to be a naturally abundant, economic, recyclable and non-toxic C<sub>1</sub> building block in organic synthesis that can occasionally replace toxic chemicals<sup>2, 3</sup>. Due to the great properties, chemical fixation of CO<sub>2</sub> becomes more and more important for decrease of carbon emission day by day<sup>4</sup>.

The most important carbon dioxide fixation products are cyclic carbonates which widely used as monomer for polymer synthesis, aprotic solvents, antifoam additives or plasticizers<sup>5-10</sup>. Cyclic carbonates can be synthesized via coupling reaction between CO<sub>2</sub> and strained heterocycles, though hard reaction conditions and often a suitable catalyst should be used<sup>11</sup>. Therefore, a variety of catalysts have been developed over the past 35 years for the synthesis of cyclic carbonates from CO<sub>2</sub> and epoxides under the leadership of Inoue and co-workers in the late 1960s<sup>12</sup>.

Among the synthesized catalysts such as alkali metal salts, transition metal complexes, Schiff Bases and ionic liquids, metal complexes based on transition metal complexes have been of great interest. We have found out that only a few metals such as Al, Cr, Co, Mg, Li, Zn, Cu and Cd are effective for coupling of

CO<sub>2</sub> and epoxides<sup>9</sup>. In recent studies, it is mentioned that transition metals Ni, Rh, Pd and Au can catalyze the same reaction<sup>13</sup>. The most distinctive advantages of the metal complexes are their easy synthesis and good stability against moisture and air. Metal complexes synthesized from these mentioned metals and salicyliminederivates have also been successfully applied as catalysts for this transformation<sup>5-8</sup>. For this purpose, the suitable ligand design for catalysts has been shown to be beneficial for the synthesis of cyclic carbonates from CO<sub>2</sub> and epoxides.

Among the various ligands, Schiff base ligands have significant importance because Schiff base ligands are potentially capable of forming stable complexes with metal ions<sup>14</sup>. By attaching donor atoms of Schiff bases, they can coordinate various metals and stabilize them in different oxidation states; such complexes are used as catalysts in many important processes<sup>15,16</sup>. The N=N bonds in azo compounds are good electron/hydrogen acceptors<sup>17</sup>. The molecule bears the azoimine (-N=N-C=N-) functional group, and is an efficient p-acid system for stabilization of low oxidation state metal ions<sup>18</sup>. Metal complexes of Schiff bases have been extensively studied at scientific applications as catalysts due to their attractive chemical and physical properties. To the best of our knowledge, Schiff base metal complexes containing azo group have not been used as catalysts for chemical fixation of carbon dioxide.

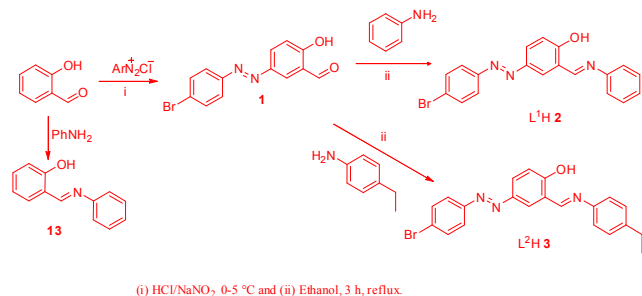
Based on this background, we decided to synthesize new Schiff base metal complexes having azo group with different transition metals such as Ni, Cu, Co, Zn and Fe in this study. There are various reported catalytic systems that are used in carbon dioxide fixation reactions. Our aim was to use azo containing NO-donor

ligands for the synthesis of cyclic carbonates from CO<sub>2</sub> and epoxides and demonstrate that the azo group has got increasing effect on the catalytic activity. Ni, Cu, Co, Zn and Fe complexes of azo containing ligands have been prepared and characterized. In addition, a Zn complex of azo free form of L<sup>1</sup>H (2) ligand 13 was prepared. These complexes were used as catalysts in direct synthesis cyclic carbonates from carbon dioxide with various epoxides. Ligand and complex structures were confirmed by, FTIR, <sup>1</sup>H-, <sup>13</sup>C- NMR, UV/Vis spectroscopy and mass spectrometry. Single-crystal X-ray analysis were performed for ligand (L<sup>1</sup>H 3) and its Zn complex 4 (Zn(L<sup>1</sup>)<sub>2</sub>). The analytical data shows that the ratio of metal to ligand in the mononuclear Schiff Base complexes is 1:2.

## 15 Result and Discussion

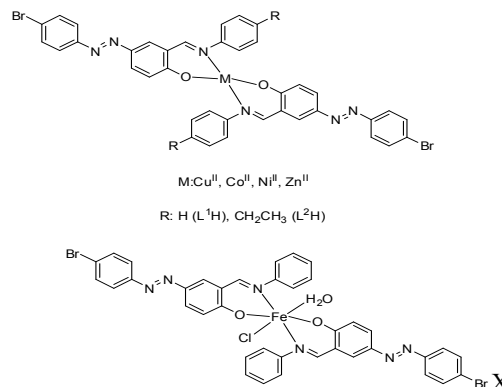
### Synthesis and characterization

The Schiff base ligands, L<sup>1</sup>H 2 and L<sup>2</sup>H 3 were prepared by the condensation of (E)-5-((4-bromophenyl)diazonyl)-2-hydroxybenzaldehyde 1 with aniline or 4-ethylaniline, respectively, (1:1 molar ratio) in EtOH as shown in Scheme 1. The level of the purity of the ligands and the complexes was checked by T.L.C. on silica gel-coated plates. Zn<sup>II</sup> 4, Co<sup>II</sup> 5, Cu<sup>I</sup> 6, Ni<sup>II</sup> 7 and Fe<sup>III</sup> 8 complexes of L<sup>1</sup>H 2 and Zn<sup>II</sup> 9, Co<sup>II</sup> 10, Cu<sup>I</sup> 11 and Ni<sup>II</sup> 12 complexes of L<sup>2</sup>H 3 were prepared.



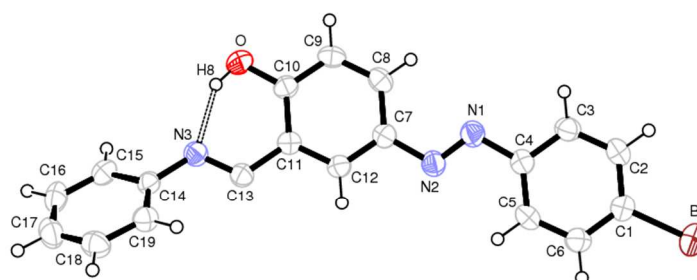
30 **Scheme 1** General synthesis of ligands

The ligands are stable at room temperature and soluble in common organic solvents such as EtOH, MeOH, DMF and CH<sub>2</sub>Cl<sub>2</sub>. The complexes are also stable at room temperature. The complexes have oxygen and nitrogen atoms as π donors and the metal ions allow π electronic delocalization as shown in Scheme 2.



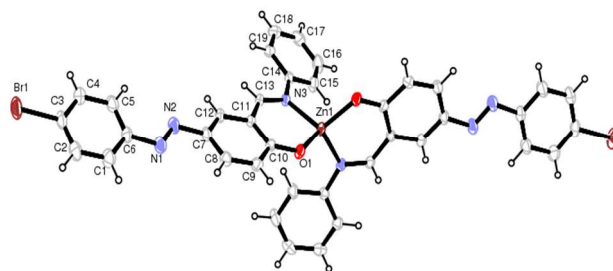
**Scheme 2** Proposed structures of metal complexes.

The structures of the complexes were further characterized by FTIR, UV-visible spectra and elemental analyses. The experimental elemental analyses results of the complexes are in good harmony with the theoretical values. The data show the complexation ratio of formulae [M(L)<sub>2</sub>] is 1:2 [Metal : Ligand]. Single crystals of L<sup>1</sup>H 2 and its Zn complex 4 which are shown in Fig. 1 and Fig. 2 were grown from DMF solutions by slow evaporation. Although the single crystals of the L<sup>2</sup>H 3 and the



other complexes were not isolated, the analytical and spectroscopic data enables us to predict possible structures as shown in Scheme 1 and 2.

50 **Fig.1** The molecular structure of L<sup>1</sup>H ligand 2, with atomic numbering scheme. The thermal ellipsoids are drawn at the 50% probability level. Dashed lines indicate the intramolecular hydrogen bond.



55 **Fig.2** The molecular structure of complex (Zn(L<sup>1</sup>)<sub>2</sub>) 4, with atomic numbering scheme. The thermal ellipsoids are drawn at the 50% probability level.

In the mass spectrum of the L<sup>1</sup>H ligand 2, the peak observed at m/z: 380 can be assigned to the molecular ions [M]<sup>+</sup>. The peaks at m/z: 169 and 210 can be attributed to the [C<sub>4</sub>H<sub>10</sub>BrN]<sup>+</sup> and [C<sub>13</sub>H<sub>10</sub>N<sub>2</sub>O]<sup>+</sup> fragments, respectively. The [M]<sup>+</sup> molecular ion

peak for the L<sup>2</sup>H ligand **3** is observed at m/z 407. The most intense peak at m/z: 311 corresponds to [C<sub>6</sub>H<sub>4</sub>-N=N-C<sub>6</sub>H<sub>3</sub>-N=CH-C<sub>6</sub>H<sub>4</sub>-C<sub>2</sub>H<sub>5</sub>]<sup>+</sup> which results from the loss of a Br atom and an OH group from the parent ligand. The mass spectra of ligands are given in Fig. S3 (ESI†).

The <sup>1</sup>H NMR spectra of the ligands are shown in Fig. S4 (ESI†). In the <sup>1</sup>H NMR spectra of the L<sup>1</sup>H **2** and L<sup>2</sup>H **3** ligands, the singlets in the 13.93–14.03 ppm range can be attributed to the proton of the first –OH group which is neighboring the azomethine group<sup>14</sup>. The <sup>1</sup>H NMR resonance of azomethine proton (CH=N) in ligands are observed at 8.76 and 8.78 ppm for L<sup>1</sup>H **2** and L<sup>2</sup>H **3** respectively. The multiplets of the aromatic protons were in the region of 8.04–7.15 and 8.11–7.16 ppm for L<sup>1</sup>H **2** and L<sup>2</sup>H **3** ligands<sup>19</sup>. The quarted signal at 2.73 ppm and the triplet signal at 1.30 ppm corresponded to –CH<sub>2</sub> and –CH<sub>3</sub> protons, respectively.

The IR spectra of the ligands and their complexes were studied and the free Schiff base ligands were compared with that of the metal complexes in order to determine the linkage of Schiff base ligands to the metal in the complexes. In the ligands and complexes spectra, both ligands, [Co(L<sup>1</sup>)<sub>2</sub>].2H<sub>2</sub>O **5** and [Fe(L<sup>1</sup>)<sub>2</sub>Cl(H<sub>2</sub>O)] **8** exhibit bands at 3409–3425 cm<sup>-1</sup> and 3075–3038 cm<sup>-1</sup> that are assignable to ν(OH) and ν(Ar-CH)<sup>20</sup>. In the complexes, the four coordination sites of metal ions were filled by two donor nitrogen and oxygen atoms. Therefore, in the complexes except for [Co(L<sup>1</sup>)<sub>2</sub>].2H<sub>2</sub>O **5** and [Fe(L<sup>1</sup>)<sub>2</sub>Cl(H<sub>2</sub>O)] **8**, the ν(OH) vibration disappeared. In the [Co(L<sup>1</sup>)<sub>2</sub>].2H<sub>2</sub>O **5** and [Fe(L<sup>1</sup>)<sub>2</sub>Cl(H<sub>2</sub>O)] **8** complex spectra, the ν(OH) vibrations that were attributed to the OH groups which were originating from H<sub>2</sub>O molecules (the presence was confirmed by elemental and thermal analyses as well). The main bands at 1621–1622 cm<sup>-1</sup> is due to the vibration of the azomethine group (-CH=N-) in L<sup>1</sup>H **2** and L<sup>2</sup>H **3** ligands<sup>21</sup>. The characteristic bands of N=N group were observed at 1567 cm<sup>-1</sup> for both ligands. Metal complexes show significant differences at vibrations as distinct from ligands. After complexation, the C=N stretching frequencies slightly shifted to lower wave number region in comparison with free ligands. The lowering in frequencies of the C=N peak suggests the formation of metal-ligand bonds. In the ranges of 417–459 and 512–663 cm<sup>-1</sup> two complementary bands were assigned to stretching vibrations ν(M-N) and ν(M-O) for the complexes<sup>22</sup>.

The electronic absorption spectral data for complexes were obtained in DMF solutions at room temperature. There are absorption bands between 642 and 211 nm for the ligands and their metal complexes at the UV–visible spectra in DMF. The chemical shift values (λ<sub>max</sub>) were determined by taking the contrast between the absorption maxima of the metal complexes and ligands. The spectra of the complexes that show intense bands in the high-energy region can be assigned to the ligand-to-metal charge transition (LMCT)<sup>23</sup>. The bands at λ<sub>max</sub> 390 and 394 nm were assigned to n→π\* transitions of the azomethine groups in the L<sup>1</sup>H **2** and L<sup>2</sup>H **3** ligands. In the spectra of the complexes, the bands of the azomethine n→π\* transitions shifted to lower frequencies indicating the involvement of the imine nitrogen atom with the metal ion. The Co<sup>II</sup> **5**, **10** complexes show bands at 458–401 and 552–639 nm. This indicates tetrahedral geometry for the Co<sup>II</sup> **5**, **10** complexes. In general, due to Jahn-Teller distortion, square planar Cu<sup>II</sup> **6**, **11** complexes give a broad absorption band

between 600 and 700 nm. Electronic spectra of the Cu<sup>II</sup> **6**, **11** complexes display bands at 642 and 639 nm<sup>6, 7</sup>. These values suggest square planar geometry for Cu<sup>II</sup> complex.

The observed magnetic moments of the Cu<sup>II</sup> complexes are 1.9–2.1 for Cu(L<sup>1</sup>)<sub>2</sub> **6** and Cu(L<sup>2</sup>)<sub>2</sub> **11** respectively which confirms that the Cu<sup>II</sup> complexes have square-planar geometry. The values of 4.7 and 4.5 B.M. reveal tetrahedral geometry around the Co<sup>II</sup> ion<sup>22</sup>. Magnetic moments measurements of Ni<sup>II</sup> **7**, **12** and Zn<sup>II</sup> **4**, **9** metal complexes show that these complexes are diamagnetic, indicating the square planar d<sup>8</sup>- and d<sup>10</sup> systems, as expected. [Fe(L<sup>1</sup>)<sub>2</sub>Cl(H<sub>2</sub>O)] **8** complex have 4.7 BM value that is equal to five unpaired electrons.

Thermal behaviors of complexes were studied using TG. and DTA. The thermal analyses were carried out in order to demonstrate the existence of water molecules in complexes [Co(L<sup>1</sup>)<sub>2</sub>].2H<sub>2</sub>O **5** and [Fe(L<sup>1</sup>)<sub>2</sub>Cl(H<sub>2</sub>O)] **8**. Thermal curves obtained for most of the complexes were very similar in character. The thermograms of complexes are shown in Fig. S5 (ESI†). Except for [Co(L<sup>1</sup>)<sub>2</sub>].2H<sub>2</sub>O **5** and [Fe(L<sup>1</sup>)<sub>2</sub>Cl(H<sub>2</sub>O)] **8** complexes, all the complexes do not show any mass losses up to 200°C, which prove that no water molecules are incorporated in complexes. The TG curve of [Co(L<sup>1</sup>)<sub>2</sub>].2H<sub>2</sub>O **5** consists mainly of three steps in the range 23–150, 150–700 and 700–1100°C. The first estimated mass loss for [Co(L<sup>1</sup>)<sub>2</sub>].2H<sub>2</sub>O **5** within the temperature range of 23–150°C may be attributed to the loss of absorbed water molecules<sup>26</sup>. Some decomposition could be correlated with proper decomposition products. The last decomposition step is in air ended with metal oxide formation. For [Fe(L<sup>1</sup>)<sub>2</sub>Cl(H<sub>2</sub>O)] **8** complex, the mass loss at 20–150°C range is assigned to losses of solvent and absorbed water molecules. Besides, this % 2 of mass loss at the range of 150–200°C is attributed to the one mol of coordinated water molecule in the complex. All the other complexes have three decomposition parts according to the losses of solvent and absorbed water molecules, decomposition of ligands and metal oxide formation, respectively. Therefore, these features confirmed the thermal stability of complex.

### Description of crystal structures

The L<sup>1</sup>H ligand **3**, crystallizes in a *monoclinic* system with the space group C<sub>c</sub> and Z=4. Individually each benzene ring in the molecule is almost planar. The C3, C12, and C18 atoms deviate from the each benzene best plane by -0.100(3), 0.016(2), and 0.0065(2) Å. All bond lengths and angles in (C1-C6), (C7-C12), and (C14-C19) benzene rings have normal values; the weighted average ring bond distances (C-C) are 1.384(4), 1.395(4), and 1.384(4) Å, respectively. The whole molecule is not planar and the P1/P2, P1/P3, and P2/P3 dihedral angles between the planes of benzene rings, respectively, P1(C1-C6), P2(C7-C12), and P3(C14-C19) are 4.73(8), 47.85(7), and 45.39(7)°. Besides the dihedral angle of P4/P5 between the planes of azo and azomethine groups [P4(C4/N1/N2/C7) and P5(C11/C13/N3/C14)] is 23.40(2)°. The two benzene rings along the N2=N1 displays trans configuration and the torsion angle of C4-N1-N2-C7 is 179.3(2)°. This angle is reported in literature as 179.80(17)<sup>027</sup>, 175.83<sup>028</sup> and 178.5(3)<sup>029</sup>. The Br-C1, N1=N2, N2-C7, and N1-C4 bond lengths are seen in Table 1, which are

values within normal ranges<sup>30</sup>.

in Table 1 for L<sup>1</sup>H 2 and Table 2 for Zn(L<sup>1</sup>)<sub>2</sub> 4, respectively.

Selected bond lengths, bond angles and torsion angles are listed

Table 1 Some selected bond lengths [Å], bond angles [°] and torsion angles [°] for L<sup>1</sup>H 2.

5

Br-C1	1.897(3)	O-C10	1.334(3)
N2-N1	1.243(3)	N2-C7	1.425(3)
C6-C5	1.371(4)	C6-C1	1.375(4)
N1-C4	1.426(3)	N3-C13	1.282(3)
N3-C14	1.413(3)	C13-C11	1.455(4)
N1-N2-C7	114.4(2)	N2-N1-C4	114.5(2)
C13-N3-C14	121.5(2)	C15-C14-N3	118.4(2)
C18-C19-C14	119.7(3)	C19-C14-N3	122.1(2)
N3-C13-C11	120.8(2)	C5-C4-N1	125.1(2)
C3-C4-N1	115.3(2)	O-C10-C11	121.8(2)
C6-C1-Br	119.3(2)	C12-C7-N2	116.6(2)
N2-N1-C4-C5	-6.2(3)	C4-N1-N2-C7	179.3(2)
N1-N2-C7-C8	10.5(3)	C13-N3-C14-C15	-146.7(2)
C14-N3-C13-C11	-170.7(2)	Br-C1-C2-C3	-179.83(19)
C2-C3-C4-N1	-177.1(2)	C8-C9-C10-O	178.9(2)
C9-C10-C11-C13	172.8(2)	O-C10-C11-C13	-6.5(3)
C13-C11-C12-C7	-171.2(2)	C10-C11-C13-N3	4.7(3)
N3-C14-C15-C16	-176.8(2)	N3-C14-C19-C18	175.5(2)

Table 2 Some selected bond lengths [Å], bond angles [°] and torsion angles [°] for Zn(L<sup>1</sup>)<sub>2</sub> 4.

Br1-C3	1.892(2)	Zn1-O1	1.9265(14)
Zn1-N3	2.0046(16)	O1-C10	1.303(2)
N1-N2	1.246(3)	N1-C6	1.432(3)
N2-C7	1.425(3)	N3-C13	1.297(2)
N3-C14	1.432(3)		
O1-Zn1-O1 <sup>i</sup>	120.43(9)	O1-Zn1-N3	98.16(6)
O1-Zn1-N3 <sup>i</sup>	109.55(6)	C10-O1-Zn1	124.25(13)
N3 <sup>i</sup> -Zn1-N3	122.69(9)	N1-N2-C7	114.5(2)
N2-N1-C6	112.5(2)	C14-N3-Zn1	121.19(12)
C13-N3-Zn1	118.73(14)		
C2-C3-Br1	118.76(19)	N3 <sup>i</sup> -Zn1-O1-C10	-130.68(15)
O1 <sup>i</sup> -Zn1-O1-C10	116.80(16)	C6-N1-N2-C7	179.20(19)
N3-Zn1-O1-C10	-1.64(16)	O1 <sup>i</sup> -Zn1-N3-C13	-123.46(14)
O1-Zn1-N3-C13	2.97(15)	O1-Zn1-N3-C14	-179.80(14)
N3 <sup>i</sup> -Zn1-N3-C13	122.54(15)	N3 <sup>i</sup> -Zn1-N3-C14	-60.22(13)
O1 <sup>i</sup> -Zn1-N3-C14	53.77(15)	N2-N1-C6-C1	173.1(2)
Br1-C3-C2-C1	-176.2(2)	N1-N2-C7-C12	173.4(2)
N2-N1-C6-C5	-7.5(3)	C12-C11-C10-O1	-178.02(19)
N1-N2-C7-C8	-7.3(3)	Zn1-N3-C14-C15	17.3(2)
C13-N3-C14-C15	-165.52(19)	Zn1-N3-C13-C11	-2.8(3)
Zn1-N3-C14-C19	-162.48(15)		

Symmetry code: (i: -x, y, -z-3/2)

In the L<sup>1</sup>H ligand **2**, a strong O-H...N intramolecular hydrogen bond is observed (Fig. 1) [O1...N3; 1.845(2) Å, O1-H8...N3; 147.00°] (Table 3) which is in good agreement with values in reported structures as 146.00°<sup>31</sup> and 147.93°<sup>29</sup>. The molecular packing of the structure is stabilized by a C-H...O intermolecular hydrogen bond and six weak C-H  $\pi$  interactions between

neighboring molecules in the unit cell (Table 3 and Fig. S1 (ESI†)). Moreover analysis of short ring-interactions shows that a considerably Cg...Cg ( $\pi$ ... $\pi$  stacking) interaction is found between Cg2...Cg2<sup>a</sup> as 4.631(13) Å [Cg2: ring (C7-C12) and symmetry code (a): x, -y, 1/2+z].

Table 3 Hydrogen bond geometry (Å, °) of compounds L<sup>1</sup>H **2** and Zn(L<sup>1</sup>)<sub>2</sub> **4**.

-	D-H...A <sup>b</sup>	D-H	H...A	D...A	D-H...A	Symmetry
L <sup>1</sup> H <b>2</b>	O1-H8...N3	0.82	1.845	2.572(3)	147.00	x, y, z
Zn(L <sup>1</sup> ) <sub>2</sub> <b>4</b>	C16-H16...Br1	0.93	2.863	3.692(3)	149.00	-1/2+x, 1/2+y, -1+z
	C19-H19...O1	0.93	2.572	3.458(3)	159.00	x, -y, 1/2+z
	C-H... $\pi$					
L <sup>1</sup> H <b>2</b>	C3-H2...R1	0.93	2.867	3.573(2)	133.65	x, -y, -1/2+z
	C6-H3...R1	0.93	2.782	3.471(2)	131.72	x, 1-y, 1/2+z
	C9-H6...R2	0.93	2.837	3.480(2)	127.25	x, -y, -1/2+z
	C12-H7...R2	0.93	2.984	3.573(2)	130.34	x, 1-y, 1/2+z
	C15-H9...R3	0.93	2.754	3.474(3)	134.83	x, 1-y, -1/2+z
	C18-H12...R3	0.93	2.805	3.534(3)	135.94	x, -y, 1/2+z
Zn(L <sup>1</sup> ) <sub>2</sub> <b>4</b>	C15-H15...R4	0.93	2.691	3.496(2)	145.36	-x, y, -1/2-z

<sup>15</sup> <sup>b</sup> D: Donor, A: Acceptor, [R1: (C1-C6), R2: (C7-C12), R3: (C14-C19) rings for L<sup>1</sup>H **2**] and [R4: (Zn1/O1/N3/C10-C13) ring for Zn(L<sup>1</sup>)<sub>2</sub> **4**].

The asymmetric unit of complex (Zn(L<sup>1</sup>)<sub>2</sub>) **4** contains one-half molecule with other half generated by an inversion centre which lies at the midpoint of Zn1 atom [symmetry code: -x, y, -z-3/2].  
<sup>20</sup> The Zn1 atom of complex (Zn(L<sup>1</sup>)<sub>2</sub>) **4** coordination geometry can be described as a distorted tetrahedral arrangement and Zn1 atom forms two six-membered chelate rings related to each other by the twofold rotation axis passing through Zn1. The dihedral angle of between these chelate rings is approximately 80.14(6)°, and the  
<sup>25</sup> Zn1-O1 and Zn1-N3 distances are 1.9265(14) and 2.0046(16) Å, close to normal values<sup>30</sup>. The defined planes A(Zn1/O1/N3/C10-C13), B(C7-C12), C(Br/N1/N2/C1-C7), and D(N3/C14-C19) are almost planar; the maximum deviations from their best planes are 0.021(2), -0.011(2), -0.064(2) and -0.002(3) Å for atoms N3,  
<sup>30</sup> C12, N1, and C16. The dihedral angles between these planes are 1.17(9), 15.36(7), 16.07(8), 14.49(9), 15.04(10), and 17.61(9)°, respectively, for A/B, A/C, A/D, B/C, B/D, and C/D. In the complex (Zn(L<sup>1</sup>)<sub>2</sub>) the two benzene rings of (C1-C6) and (C7-C12) adopt a trans configuration with respect to N1=N2 double  
<sup>35</sup> bond and the torsion angle of C6-N1-N2-C7 is 179.20(19)°. The molecules are linked by C-H...Br and C-H...O hydrogen bonds forming a three-dimensional network (Table 3 and Fig.S2 (ESI†)). Besides a weak C-H... $\pi$  interaction are present in the

<sup>40</sup> unit cell and listed in Table 3.

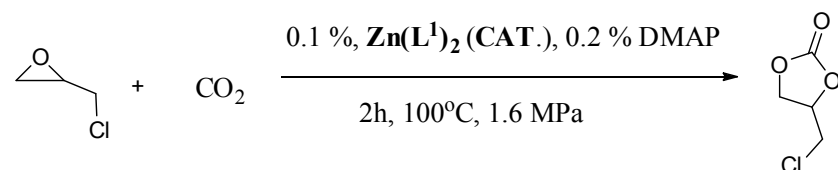
### Catalytic studies

The carboxylation of epichlorohydrin with CO<sub>2</sub> into corresponding cyclic carbonate (4-(chloromethyl)-1,3-dioxolan-  
<sup>45</sup> 2-one) in the presence of 0.1% complexes were conducted in a batch-wise operation under various conditions as shown in Table 4. The coupling of carbon dioxide and various epoxides catalyzed by complexes were investigated under different reaction conditions (Table 4, entries 1-9). Catalytic experiments were  
<sup>50</sup> carried out at optimized conditions, which were determined at our previous studies<sup>32-35</sup>. Five different types of organic bases were used as co-catalysts. Also, two different types of ionic liquids (IL) as catalysts were investigated. One is the 1-Butyl-3-methylimidazolium iodide ((bmim)I) and the other one is 1-  
<sup>55</sup> Butyl-3-methylimidazolium hexafluorophosphate ((bmim)PF<sub>6</sub>).

Cite this: DOI: 10.1039/c0xx00000x

www.rsc.org/xxxxxx

## ARTICLE TYPE

Table 4 Synthesis of ECHC (4-(chloromethyl)-1,3-dioxolan-2-one) from ECH (2-(chloromethyl)oxirane) and CO<sub>2</sub> catalyzed by metal complexes.

Entry	Cat.	Yield <sup>a</sup> (%)	Selectivity <sup>a</sup> (%)	TON <sup>b</sup>	TOF <sup>c</sup> (h <sup>-1</sup> )
Blank	Zn(L <sup>1</sup> ) <sub>2</sub> <b>4</b>	3.0 <sup>d</sup>	92.0	30	15
1	Zn(L <sup>1</sup> ) <sub>2</sub> <b>4</b>	62.1	98.2	621	311
2	Zn(L <sup>2</sup> ) <sub>2</sub> <b>9</b>	51.4	99.3	514	257
3	Cu(L <sup>1</sup> ) <sub>2</sub> <b>6</b>	48.0	97.4	480	240
4	Cu(L <sup>2</sup> ) <sub>2</sub> <b>11</b>	50.6	97.4	506	253
5	Ni(L <sup>1</sup> ) <sub>2</sub> <b>7</b>	54.5	98.4	545	273
6	Ni(L <sup>2</sup> ) <sub>2</sub> <b>12</b>	49.3	98.6	493	247
7	[Co(L <sup>1</sup> ) <sub>2</sub> ].2H <sub>2</sub> O <b>5</b>	27.9	98.5	279	140
8	Co(L <sup>2</sup> ) <sub>2</sub> <b>10</b>	55.7	98.9	557	279
9	[Fe(L <sup>1</sup> ) <sub>2</sub> Cl(H <sub>2</sub> O)] <b>8</b>	52.1	97.2	521	261

**Reaction conditions:** Cat.(4.5x10<sup>-5</sup>mol), epichlorohydrin (4.5x10<sup>-2</sup>mol),DMAP (9x10<sup>-5</sup>mol), CO<sub>2</sub> (1.6 MPa), 100 °C, 2 h.

<sup>d</sup>Cat.(4.5x10<sup>-5</sup>mol), epichlorohydrin (4.5x10<sup>-2</sup>mol), CO<sub>2</sub> (1.6 MPa), 100 °C, 2 h.

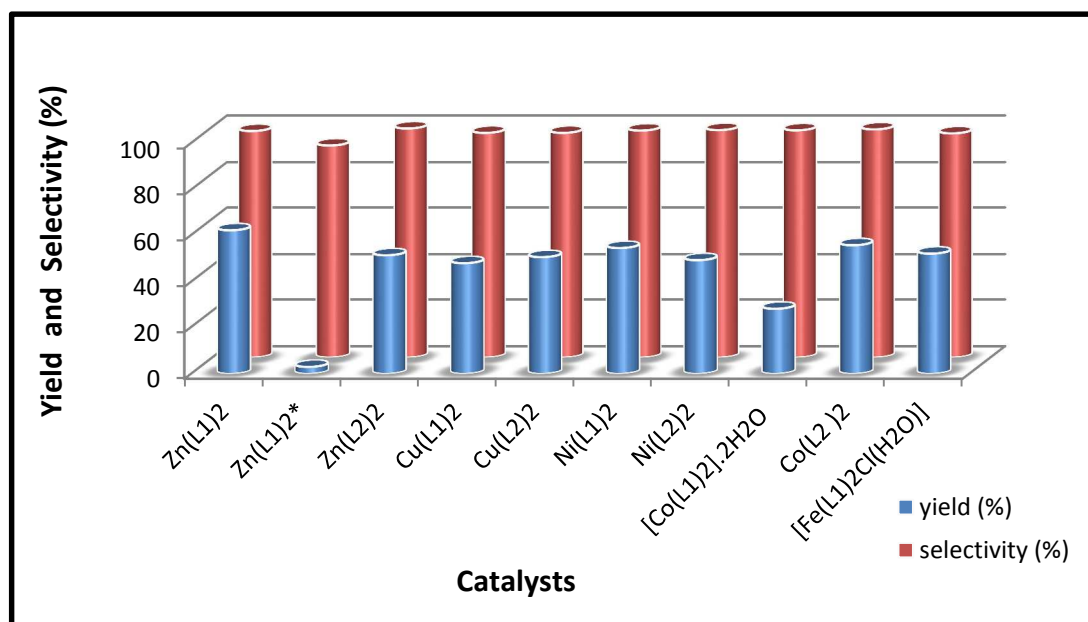
<sup>a</sup>Yield and selectivity of epichlorohydrin to corresponding cyclic carbonate were determined by GC.

<sup>b</sup>Moles of cyclic carbonate produced per mole of catalyst.

<sup>c</sup>The rates expressed in terms of the turnover frequency {TOF [mol of product (mol of catalyst h)<sup>-1</sup>]=turnovers/h}

<sup>20</sup> The complexes, when used 4-dimethylamino pyridine (DMAP) as co-catalyst, showed highest catalytic activity and selectivity for the conversion of CO<sub>2</sub> into cyclic carbonates using the epoxide derivatives which served as substrate and solvent. The complex **4**

<sup>25</sup> (Zn(L<sup>1</sup>)<sub>2</sub>)bearing phenylimino group and DMAP showed best catalytic activity and selectivity (yield: 62.1% and selectivity: 98.2%) for the coupling of CO<sub>2</sub> and epichlorohydrin as substrate (Fig. 3).



<sup>30</sup>

\*Zn(L<sup>1</sup>)<sub>2</sub> **4** (4.5x10<sup>-5</sup>mol), epichlorohydrin (4.5x10<sup>-2</sup>mol), CO<sub>2</sub> (1.6 MPa), 100 °C, 2 h.

**Fig. 3** The effects of catalysts for the formation of epichlorohydrin to corresponding cyclic carbonate at the same catalytic conditions.

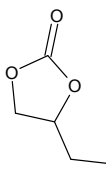
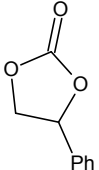
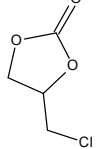
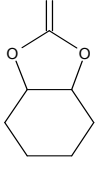
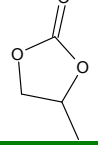
Interestingly, excluding complex  $Zn(L^1)_2$  **4**, the activities of catalysts were significantly low. Lots of parameters such as solubility of complexes in epoxide, polarity, biphasic reaction media, differences between catalysts and substrates could play a role for this phenomenon.

### Synthesis of cyclic carbonates from other epoxides and $CO_2$

The above results indicate that complex  $Zn(L^1)_2$  **4** is an efficient catalyst for the cycloaddition of  $CO_2$  to ECH. For investigation of the efficiency of the catalytic system, different epoxides (epichlorohydrin (ECH), 1,2-epoxybutane (EB), Propylene oxide

(PO), styrene oxide (SO) and cyclohexene oxide (CHO)) were used as both solvent and substrate under optimized reaction conditions. As shown in Table 5, epichlorohydrin was found to be the most reactive epoxide, while cyclohexene oxide exhibited the lowest activity of the epoxides surveyed. This result may be due to more electron donating substituents linked to  $C_2$ -atom of these epoxides (EB, SO, PO and CHO) which could be coordinated to the metal centre and was responsible for the catalyst poisoning<sup>35</sup>. The results of optimization conditions such as reaction temperature, epoxide, time and  $CO_2$  pressure were very similar for both homogeneous and heterogeneous systems that were previously reported<sup>36</sup>.

Table 5 The comparison of various epoxides to corresponding cyclic carbonates at the same catalytic conditions with  $Zn(L^1)_2$  **4** catalyst

Entry	Product	Yield <sup>a</sup> (%)	Selectivity <sup>a</sup> (%)	Entry	Product	Yield <sup>a</sup> (%)	Selectivity <sup>a</sup> (%)
1		3.3	99.0	4		2.4	95.8
2		62.1	98.2	5		0.6	72.5
3		4.2	73.2				

<sup>a</sup>Yield and selectivity of epichlorohydrin to corresponding Epichlorohydrin carbonate were determined by GC.

<sup>b</sup>Reaction conditions: epoxides ( $4.5 \cdot 10^{-2}$  mol), catalyst:  $Zn(L^1)_2$  ( $4.5 \cdot 10^{-5}$  mol), DMAP ( $9 \cdot 10^{-5}$  mol),  $100^\circ C$ , 1.6 MPa and 2 h.

### Influence of bases on the ECHC (4-(chloromethyl)-1,3-dioxolan-2-one) synthesis

We also evaluated the effect of co-catalyst on the catalytic performance (Fig. 4). For this purpose, organic bases (DMAP (4-(dimethylamino)pyridine),  $CH_3CN$  (acetonitrile),  $C_5H_5N$  (pyridine),  $NEt_3$  (triethylamine) and  $PPh_3$  (triphenylphosphine)) were used as co-catalyst. Interestingly, the use of  $CH_3CN$  resulted in the yield of 1.3%, and the yield remarkably increased up to 62.1% when DMAP was used as the base in high selectivity<sup>37</sup>.

Pyridine based co-catalyst systems ( $C_5H_5N$  and DMAP) were found to be effective bases. Especially, DMAP which has *N*-dimethyl amino moiety showed the best activity. The catalytic efficiencies of these co-catalysts were found to be in the following order:  $CH_3CN < PPh_3 < NEt_3 < C_5H_5N < DMAP$ . Similar effect was observed in our previous papers<sup>40</sup>. Blank reaction was made to determine the effect of co-catalyst (Table 4, Blank run). Consequently, the necessity of base was observed as shown in Fig. 4.



Cite this: DOI: 10.1039/c0xx00000x

www.rsc.org/xxxxxx

ARTICLE TYPE

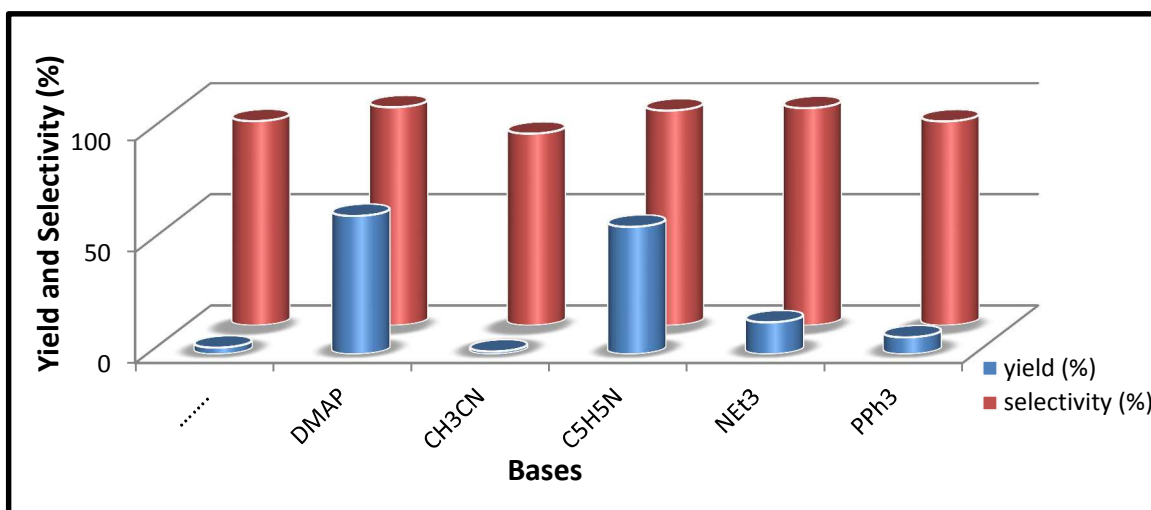


Fig. 4 Conversion and selectivity of 2-(chloromethyl)oxirane as a function of base at the same catalytic conditions with  $Zn(L^1)_2$  4 catalyst.

#### Optimization Studies

Since the  $Zn(L^1)_2$  4 showed good catalytic activity, the effects of reaction parameters (temperature,  $CO_2$  pressure, and time) were examined using this catalytic system. Firstly, the effect of reaction time on the ECHC yield was investigated. Fig. 5 shows that the ECHC yield increased with reaction time up to a period

10 4h. It is observed that the cycloaddition reaction proceeds rapidly within the first 2 h, reaching an ECHC yield of 62.1%. Following an increase in time from 0.5 to 4h, ECHC yield increased sharply from 29.5 to 65.5% (Fig. 5). On this basis, the experiments to assess other reaction parameters were performed for 2h.

15

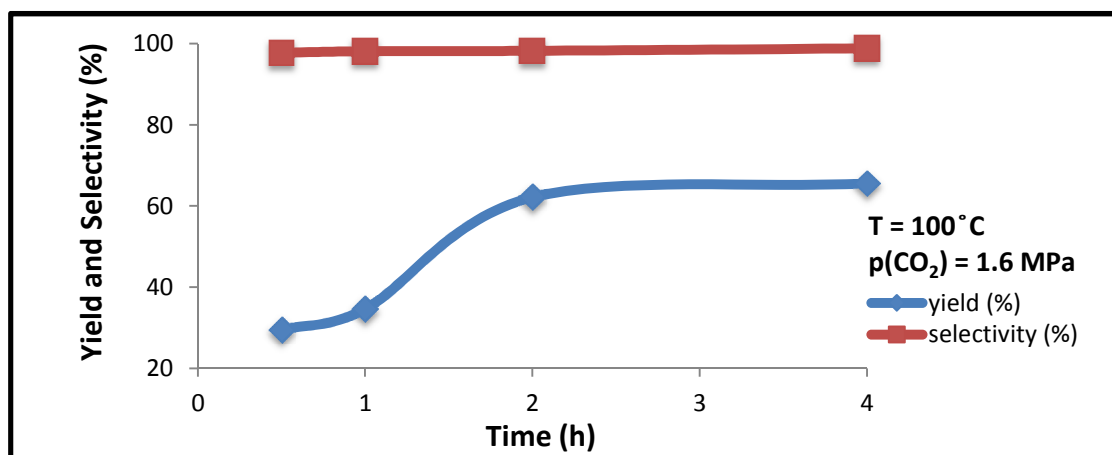


Fig. 5 Conversion and selectivity of ECH as a function of time with  $Zn(L^1)_2$  4 as catalyst.

The results shown in Fig. 6 clearly show that temperature has a strong effect on the ECH conversion. When catalytic reactions were conducted at 75, 100, 125, and 150 °C, the ECH conversions were 11.9, 62.1, 91.8, and 93.9%, respectively. With increase of temperature from 75 to 125 °C, ECHC yield increased sharply

from 11.9 to 91.8%. With increase of temperature from 125 to 150 °C, ECHC yield slowly increased from 91.8 to 93.9% (Fig. 13). This temperature and conversion relationship is attributed to higher reactivity at a higher temperature. These types of catalysts were found to be more reactive at high temperatures. As a result, the temperature is required for these catalysts (Fig. 6).

Cite this: DOI: 10.1039/c0xx00000x

www.rsc.org/xxxxxx

ARTICLE TYPE

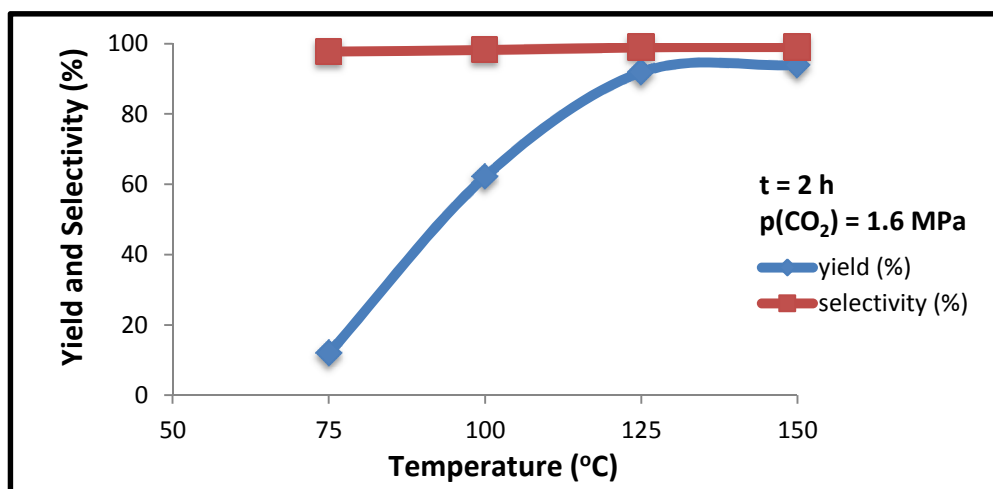


Fig. 6 Conversion and selectivity of ECH as a function of temperature with  $\text{Zn}(\text{L})_2 \mathbf{4}$  as catalyst.

The effects of  $\text{CO}_2$  pressure were also investigated. As shown in Fig. 7, in the low-pressure range (0.5-1.6 MPa), there has been a rise in ECHC yield (from 32.4% to 62.1%) with an increase in initial  $\text{CO}_2$  pressure. But, further rise of pressure to 4 MPa results in moderate decrease in ECHC yield (from 62.1% to 38.6%). Similar effects of  $\text{CO}_2$  pressure on catalytic activity were observed in our previous reports<sup>32</sup>. In a catalytic reaction system, a higher  $\text{CO}_2$  pressure can effectively increase the solubility of  $\text{CO}_2$  in ECH, enabling the reaction equilibrium to shift toward carbonate formation. However, when  $\text{CO}_2$  pressure reached 4 MPa, this high  $\text{CO}_2$  pressure may have retarded the interaction

between ECH and catalysts, resulting in a decrease in ECH conversion. Thus, the best EC yield could be achieved at 1.6 MPa. According to the literature, this can be explained qualitatively by the effect of pressure on the concentration of  $\text{CO}_2$  and epoxide in the two phases in the reaction systems<sup>41</sup>. The upper phase is the vapour phase, and bottom phase is the liquid phase. The reaction took place mainly in the liquid phase because the catalyst was dispersed in the liquid phase. When the pressure was higher than 4 MPa, the  $\text{CO}_2$  concentration was too high and inhibited the contact of ECH with the catalyst by a dilution effect<sup>41-46</sup>.

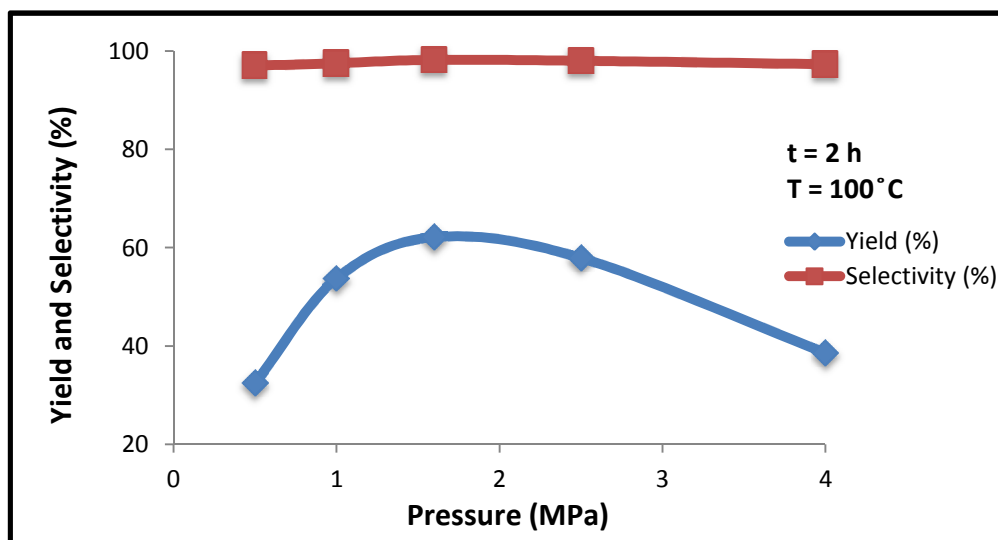


Fig. 7 Conversion and selectivity of ECH as a function of pressure with  $\text{Zn}(\text{L})_2 \mathbf{4}$  as catalyst.

Cite this: DOI: 10.1039/c0xx00000x

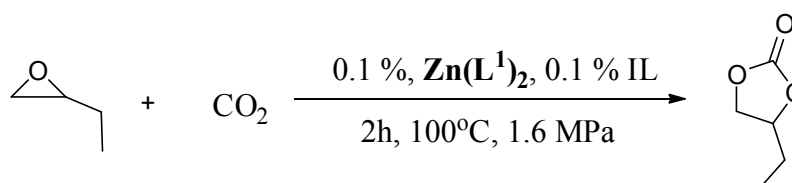
www.rsc.org/xxxxxx

## ARTICLE TYPE

**Synthesis of cyclic carbonates from EB and CO<sub>2</sub> catalyzed by metal complexes and ionic liquids.**

The carboxylation of epoxybutane with CO<sub>2</sub> into corresponding cyclic carbonate (4-ethyl-1,3-dioxolan-2-one) in the presence of 0.1% catalyst system was conducted in a batch-wise operation under various conditions as shown in Table 6, entries 1-5. In this study, two different types of ionic liquids (IL) as catalysts were

investigated. One is the (bmim)I (1-butyl-3-methylimidazolium iodide) and the other one is (bmim)PF<sub>6</sub> (1-butyl-3-methylimidazolium hexafluorophosphate). The best active complex compound (Zn(L<sup>1</sup>)<sub>2</sub> **4**) and ionic liquids ((bmim)I and (bmim)PF<sub>6</sub>) were used together as binary catalytic system and their activities were investigated. Ionic liquids, metal complexes and the binary catalytic system were compared for each catalytic condition (Fig. 8).

Table 6 Synthesis of EBHC (4-ethyl-1,3-dioxolan-2-one) from EB (2-ethyloxirane) and CO<sub>2</sub> catalyzed by metal complexes and ionic liquids.

20

Entry	Cat.	Yield <sup>a</sup> (%)	Selectivity <sup>a</sup> (%)	TON <sup>b</sup>	TOF <sup>c</sup> (h <sup>-1</sup> )
1	Zn(L <sup>1</sup> ) <sub>2</sub> <b>4</b>	62.1 <sup>d</sup>	98.2	621	311
2	(bmim)I	85.0	97.0	85.0	43
3	(bmim)PF <sub>6</sub>	83.6	99.0	83.6	41.8
4	(bmim)I+Zn(L <sup>1</sup> ) <sub>2</sub> <b>4</b>	89.7	91.8	89.7	44.9
5	(bmim)PF <sub>6</sub> +Zn(L <sup>1</sup> ) <sub>2</sub> <b>4</b>	94.3	94.6	94.3	47.2

25

**Reaction conditions:** Cat.(4.5x10<sup>-5</sup>mol), IL(4.5x10<sup>-5</sup>mol), 1,2- epoxybutane (4.5x10<sup>-3</sup>mol), CO<sub>2</sub> (1.6 MPa), 100 °C, 2 h.

<sup>d</sup>Cat.(4.5x10<sup>-5</sup>mol), 1,2- epoxybutane (4.5x10<sup>-2</sup>mol), DMAP (9x10<sup>-5</sup>mol), CO<sub>2</sub> (1.6 MPa), 100 °C, 2 h.

<sup>a</sup>Yield and selectivity of epoxybutaneto corresponding epoxybutane carbonate were determined by GC.

<sup>b</sup>Moles of cyclic carbonate produced per mole of catalyst.

<sup>c</sup>The rates expressed in terms of the turnover frequency {TOF [mol of product (mol of catalyst h<sup>-1</sup>)]=turnovers/h}

35

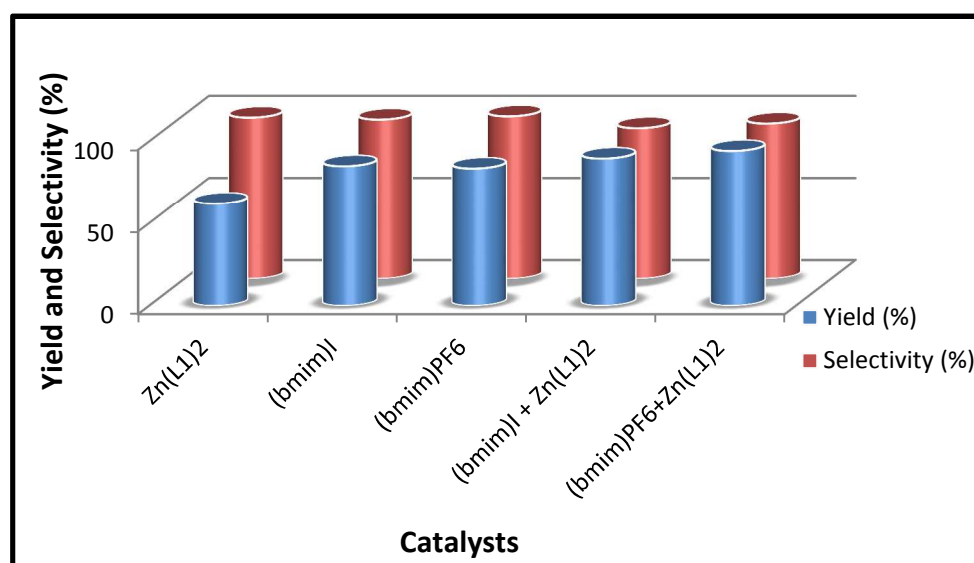


**Fig. 8** The effects of catalysts for the formation of epoxybutane to corresponding cyclic carbonate at the same catalytic conditions.

The (bmim)PF<sub>6</sub><sup>+</sup> Zn(L<sup>1</sup>)<sub>2</sub> **4** as binary catalytic system showed the best catalytic activity and selectivity (yield: 94.3% and selectivity: 94.6%) for the coupling of CO<sub>2</sub> and epoxybutane (Table 6, entry 5). The similar Salen type Zn(II) complex which has not involved the azo-moieties **13** has been prepared and tested at the same catalytic conditions to see the effectiveness of the azo-moieties. The %43.2 yield was achieved with 97.9% selectivity. This result shows that, azo-moiety has positive affect to the catalytic system.

## Experimental

### Materials and measurements

All solvents were of reagent grade. The metal salts [Zn(CH<sub>3</sub>COO)<sub>2</sub>H<sub>2</sub>O, Cu(CH<sub>3</sub>COO)<sub>2</sub>H<sub>2</sub>O, Ni(Cl)<sub>2</sub>.6H<sub>2</sub>O, Co(CH<sub>3</sub>COO)<sub>2</sub>.4H<sub>2</sub>O, Fe(Cl)<sub>3</sub>.6H<sub>2</sub>O], *p*-bromoaniline, aniline, 4-ethylaniline and salicylaldehyde were obtained from Fluka.

Elemental analyses were carried out by The Scientific and Technological Research Center of İnönü University. IR spectra were obtained using KBr discs (4000–400 cm<sup>-1</sup>) on a Shimadzu

Table 7 Crystal data and structure refinements for ligand (L<sup>1</sup>H **2**) and complex (Zn(L<sup>1</sup>)<sub>2</sub> **4**).

8300 FTIR spectrophotometer. The electronic spectra in the 200–900 nm range were obtained using DMF on a Hithachi U-3900 spectrophotometer. Magnetic measurements were carried out by the Gouy method using MnCl<sub>2</sub> as calibrant. ESI mass spectra were recorded on a ESI/MS Tandem mass spectrometry. <sup>1</sup>H and <sup>13</sup>C NMR spectra were recorded on a Varian AS-400 MHz instrument and Bruker 600 MhzUltrashield TM in CDCl<sub>3</sub>. The diffraction data for suitable single crystals of L<sup>1</sup>H **3** ligand and its Zn<sup>II</sup> complex **4** (Zn(L<sup>1</sup>)<sub>2</sub>) were collected using a Bruker APEX-II CCD diffractometer equipped with a MoK<sub>α</sub> radiation source (λ=0.71073Å at 296 K). ω/2θ scan mode was employed for data collection. The structures were solved by SHELXS-97<sup>38</sup> and refined with SHELXL-97<sup>39</sup> software package. All non-hydrogen atoms were assigned anisotropic displacement parameters and refined positional constraints. The H atoms were placed in geometrically idealized positions, with C-H distances of 0.93 Å (aromatic) for L<sup>1</sup>H**2** and Zn(L<sup>1</sup>)<sub>2</sub> **4**, and 0.82 Å (hydroxyl) for L<sup>1</sup>H **2**. Details of the data collection parameters and crystallographic information for L<sup>1</sup>H and Zn(L<sup>1</sup>)<sub>2</sub> are given in Table 7.

Properties	L <sup>1</sup> H <b>2</b>	Zn(L <sup>1</sup> ) <sub>2</sub> <b>4</b>
Empirical Formula	C <sub>19</sub> H <sub>13</sub> BrN <sub>3</sub> O	C <sub>38</sub> H <sub>26</sub> Br <sub>2</sub> N <sub>6</sub> O <sub>2</sub> Zn
Formula weight	379.23	823.84
Crystal system	Monoclinic	Monoclinic
Space group	Cc	C2/c
Unit cell dimensions	a = 37.4840(11) Å b = 7.0935(2) Å c = 6.2089(2) Å β = 97.497(2) <sup>o</sup>	a = 34.9897(7) Å b = 8.3586(2) Å c = 11.8489(3) Å β = 105.3030(10) <sup>o</sup>
Volume	1636.79(8) Å <sup>3</sup>	3342.52(13) Å <sup>3</sup>
Z	4	8
Calculated density	1.539 Mg/m <sup>3</sup>	1.637 Mg/m <sup>3</sup>
Absorption coefficient	2.522 mm <sup>-1</sup>	3.171 mm <sup>-1</sup>
F(000)	764	1648
Crystal size	0.45 x 0.23 x 0.04 mm	0.45 x 0.25 x 0.10 mm
θ range for data collection	2.19–26.37 <sup>o</sup>	2.41–30.27 <sup>o</sup>
Limiting indices	-46 ≤ h ≤ 46 -8 ≤ k ≤ 8 -7 ≤ l ≤ 7	-49 ≤ h ≤ 47 -11 ≤ k ≤ 11 16 ≤ l ≤ 16
Reflections collected	9427	19157
Unique reflections	2858 [R(int) = 0.0323]	4951 [R(int)=0.0322]
Completeness to theta	26.37 99.3 %	30.27 99.0 %
Max. and min. Transmission	0.9059 and 0.3966	0.7422 and 0.3295
Refinement method	Full-matrix least-squares on F <sup>2</sup>	Full-matrix least-squares on F <sup>2</sup>
Data / restraints / parameters	2858 / 0 / 217	4951 / 0 / 222
Goodness-of-fit on F <sup>2</sup>	1.008	1.018
Final R indices [I > 2σ(I)]	R <sub>1</sub> =0.0289, wR <sub>2</sub> =0.0626	R <sub>1</sub> =0.0380, wR <sub>2</sub> =0.0832
R indices (all data)	R <sub>1</sub> =0.0334, wR <sub>2</sub> =0.0643	R <sub>1</sub> =0.0729, wR <sub>2</sub> = 0.0945

$\Delta\rho_{\max}$  and  $\Delta\rho_{\min}$ 0.343 and -0.184 e. Å<sup>-3</sup>0.662 and -0.515 Å<sup>-3</sup>

Selected bond lengths, bond angles and torsion angles are listed in Table 1 for L<sup>1</sup>H **2** and Table 2 for Zn(L<sup>1</sup>)<sub>2</sub> **4**, respectively. Hydrogen bonding geometries of L<sup>1</sup>H **2** and Zn(L<sup>1</sup>)<sub>2</sub> **4** are shown in Table 3. The ORTEP<sup>40</sup> drawings of the molecule indicating atom numbering scheme with thermal ellipsoids at %50 probability are given in Fig. 1 for L<sup>1</sup>H **2** and Fig.4 for Zn(L<sup>1</sup>)<sub>2</sub> **4**. The PARST<sup>47</sup> and PLATON<sup>48</sup> programs were used for geometrical calculation and conformational features of the molecules. Further experimental details have been deposited as supplementary material at the Cambridge Crystallographic Data Centre CCDC 1035285-1035286.

The yields of epoxides to corresponding cyclic carbonates were determined by GC (Agilent 7820A) with HP-5 MS column.

#### Synthesis of (E)-5-((4-bromophenyl)diazenyl)-2-hydroxybenzaldehyde **1**

(E)-5-((4-bromophenyl)diazenyl)-2-hydroxybenzaldehyde **1** was prepared according to the reported procedure<sup>49</sup>.

#### Synthesis of 4-((E)-(4-bromophenyl)diazenyl)-2-((E)-(phenylimino)methyl)phenol **2** (L<sup>1</sup>H)

4-((E)-(4-bromophenyl)diazenyl)-2-((E)-(phenylimino)methyl)phenol **2** (L<sup>1</sup>H) (Scheme 1) was synthesized as follow; 10 mmol (3.05 g) of (E)-5-((4-bromophenyl)diazenyl)-2-hydroxybenzaldehyde **1** and 10 mmol (0.93 g) of aniline were condensed by refluxing in 70 cm<sup>3</sup> of absolute ethanol for 3 h. The solution was left at room temperature. 4-((E)-(4-bromophenyl)diazenyl)-2-((E)-(phenylimino)methyl)phenol **2** was obtained as orange micro crystals; the micro crystals were filtered off, washed with 10 cm<sup>3</sup> of absolute ethanol and then recrystallized from DMF. Yield: 7.8 g (79%). Anal. Calcd. (%) for C<sub>19</sub>H<sub>14</sub>BrN<sub>3</sub>O (*M*= 380.24): C 60.00, H 3.69, N 11.05. Found (%): C 60.02, H 3.71, N 11.05. FT-IR (cm<sup>-1</sup>, KBr): 3434 (s), 3075 (s), 1621 (s), 1567 (s). UV-Vis (λ, nm): 224, 277, 335, 390. <sup>1</sup>H NMR (400 MHz, CDCl<sub>3</sub>δppm): 13.93 (bs, 1H), 8.76 (s, 1H), 8.04 (m, 2H), 7.79 (m, 2H), 7.66 (m, 2H), 7.47 (m, 2H), 7.34 (m, 3H), 7.15 (d, *J* = 8.8 Hz, 1H). <sup>13</sup>C NMR (101 MHz, CDCl<sub>3</sub>δppm): 164.4, 162.0, 151.3, 147.7, 145.4, 132.3, 129.6, 128.2, 127.5, 127.4, 124.8, 124.1, 121.2, 118.9, 118.3. MS *m/z*: 380 [M]<sup>+</sup>.

#### Synthesis of 4-((E)-(4-bromophenyl)diazenyl)-2-((E)-(4-ethylphenyl)imino)methyl)phenol **3** (L<sup>2</sup>H)

10 mmol (3.05 g) of (E)-5-((4-bromophenyl)diazenyl)-2-hydroxybenzaldehyde **1** and 10 mmol (1.21 g) of 4-ethylaniline were condensed by refluxing in 50 cm<sup>3</sup> of absolute EtOH for 3 h. The solution was left at room temperature. The product was obtained as orange micro crystals; the micro crystals were filtered off, washed with 10 cm<sup>3</sup> of absolute ethanol and dried in air. Yield: 8.2 g (75%). Anal. Calcd. (%) for C<sub>21</sub>H<sub>18</sub>BrN<sub>3</sub>O (*M*=

408.30): C 61.70, H 4.41, N 10.28. Found (%): C 61.78, H 4.44, N 10.29. FT-IR (cm<sup>-1</sup>, KBr): 3445 (s), 3055 (s), 1622 (s), 1567 (s). UV-Vis (λ, nm): 234, 292, 346, 394. <sup>1</sup>H NMR (600 MHz, CDCl<sub>3</sub>δppm): 14.03 (s, 1H), 8.78 (s, 1H), 8.11 – 8.01 (m, 2H), 7.83 – 7.75 (m, 2H), 7.70 – 7.62 (m, 2H), 7.29 (m, 4H), 7.16 (d, *J* = 8.7 Hz, 1H), 2.73 (q, *J* = 7.6 Hz, 2H), 1.30 (t, *J* = 7.6 Hz, 3H). <sup>13</sup>C NMR (101 MHz, CDCl<sub>3</sub>δppm): 164.52, 160.98, 151.38, 145.37, 145.21, 143.91, 132.30, 128.97, 128.03, 127.31, 124.75, 124.10, 121.13, 119.02, 118.28, 28.50, 15.56. MS *m/z*: 407 [M]<sup>+</sup>.

#### Synthesis of (E)-2-((phenylimino)methyl)phenol **13**

(E)-2-((phenylimino)methyl)phenol **13** was prepared according to the literature<sup>50</sup>.

25 mL 2-hydroxybenzaldehyde (508.5 mg, 2.00mmol) solution in methanol was added aniline (186.3 mg, 2 mmol) in methanol (50 mL) and refluxed for 8 hours. The solution was concentrated on air by removing solvent for two days and crystallized to give (E)-2-((phenylimino)methyl)phenol **13** as a yellow needle crystals. Yield: 5.5 g (83%). Anal. Calcd. (%) for C<sub>13</sub>H<sub>11</sub>NO (*M*= 197.2): C 79.16, H 5.62, N 7.10. Found (%): C 78.93, H 5.71, N 7.05. FT-IR (cm<sup>-1</sup>, KBr): 3430 (s), 3060 (s), 1600 (s). UV-Vis (λ, nm): 275, 339, 393.

#### General procedure for the synthesis of metal complexes

L<sup>1</sup>H **2** and L<sup>2</sup>H **3** ligands (20 mmol) dissolved in 200 cm<sup>3</sup> absolute EtOH was mixed with 10 mmol metal salts in 10 cm<sup>3</sup>EtOH. The stirred mixture was refluxed for 24 h, then evaporated to 15–20 cm<sup>3</sup> in vacuum and left to cool to room temperature. The compounds were precipitated after adding 5 cm<sup>3</sup> EtOH. The products were filtered in vacuum, washed with a small amount of MeOH and water. Zn(L<sup>1</sup>)<sub>2</sub> **4** recrystallized from DMF. The products are soluble in solvents such as CHCl<sub>3</sub>, DMF and DMSO.

Zn(L<sup>1</sup>)<sub>2</sub> (**4**): Yield: 6.8 g (83%). Anal. Calcd. (%) for C<sub>38</sub>H<sub>26</sub>Br<sub>2</sub>N<sub>6</sub>O<sub>2</sub>Zn (*M*= 823,84): C 55.43, H 3.15, N 10.19. Found (%): C55.40, H3.18, N 10.20. FT-IR (cm<sup>-1</sup>, KBr): 3038 (s), 1607 (s), 1585 (s), 528 (w), 422 (w). UV-Vis (λ, nm): 283, 333, 399, 457.

[Co(L<sup>1</sup>)<sub>2</sub>].2H<sub>2</sub>O (**5**): Yield: 6.1 g (72%). Anal. Calcd. (%) for C<sub>38</sub>H<sub>30</sub>Br<sub>2</sub>N<sub>6</sub>O<sub>4</sub>Co (*M*= 853.42): C 53.48, H 3.54, and N 9.85. Found (%): C 53.04, H 3.15, N 9.70. FT-IR (cm<sup>-1</sup>, KBr): 3412 (s), 3038 (s), 1613 (s), 1585 (s), 594 (w), 418 (w). UV-Vis (λ, nm): 237, 279, 348, 366, 458, 552.

Cu(L<sup>1</sup>)<sub>2</sub> (**6**): Yield: 6.7 g (81%). Anal. Calcd. (%) for C<sub>38</sub>H<sub>26</sub>Br<sub>2</sub>N<sub>6</sub>O<sub>2</sub>Cu (*M*= 822,01): C 55.74, H 3.45, N 10.22. Found (%): C 55.52, H 3.19, N 10.22. FT-IR (cm<sup>-1</sup>, KBr): 3041 (s), 1602 (s), 1528 (s), 599 (w), 457 (w). UV-Vis (λ, nm): 236, 275, 335, 366, 425, 642.

Ni(L<sup>1</sup>)<sub>2</sub> (**7**): Yield: 6.5 g (79%). Anal. Calcd. (%) for C<sub>38</sub>H<sub>26</sub>Br<sub>2</sub>N<sub>6</sub>O<sub>2</sub>Ni (*M*= 817,15): C 55.25, H 3.22, N 10.18. Found (%): C 55.85, H 3.21, N 10.28. FT-IR (cm<sup>-1</sup>, KBr): 3048 (s), 1601

(s), 1595 (s), 515 (w), 459 (w). UV-Vis ( $\lambda$ , nm): 283, 375, 490, 539.

**[Fe(L<sup>1</sup>)<sub>2</sub>Cl(H<sub>2</sub>O)] (8):** Yield: 7.4 g (85%). Anal. Calcd. (%) for C<sub>38</sub>H<sub>28</sub>Br<sub>2</sub>N<sub>6</sub>O<sub>3</sub>Co (*M*= 867.77): C 52.46, H 3.27, N 9.58. Found (%) : C 52.60, H 3.25, N 9.68. FT-IR (cm<sup>-1</sup>, KBr): 3403 (s), 3056 (s), 1607 (s), 1599 (s), 589 (w), 425 (w). UV-Vis ( $\lambda$ , nm): 270, 330, 350, 375, 610.

**Zn(L<sup>2</sup>)<sub>2</sub> (9):** Yield: 7.6 g (87%). Anal. Calcd. (%) for C<sub>42</sub>H<sub>34</sub>Br<sub>2</sub>N<sub>6</sub>O<sub>2</sub>Zn (*M*= 879.95): C 57.29, H 3.90, N 9.52. Found (%) : C 57.33, H 3.92, N 9.55. FT-IR (cm<sup>-1</sup>, KBr): 3058 (s), 1609 (s), 1579 (s), 587 (w), 418 (w). UV-Vis ( $\lambda$ , nm): 276, 359, 414, 507.

**Co(L<sup>2</sup>)<sub>2</sub> (10):** Yield: 6.5 g (75%). Anal. Calcd. (%) for C<sub>42</sub>H<sub>34</sub>Br<sub>2</sub>N<sub>6</sub>O<sub>2</sub>Co (*M*= 873.50): C 57.60, H 3.92, N 9.60. Found (%) : C 57.75, H 3.92, N 9.62. FT-IR (cm<sup>-1</sup>, KBr): 3062 (s), 1602 (s), 1576 (s), 610 (w), 420 (w). UV-Vis ( $\lambda$ , nm): 235, 280, 348, 366, 545.

**Cu(L<sup>2</sup>)<sub>2</sub> (11):** Yield: 7.5 g (85%). Anal. Calcd. (%) for C<sub>42</sub>H<sub>34</sub>Br<sub>2</sub>N<sub>6</sub>O<sub>2</sub>Cu (*M*= 878.11): C 57.21, H 3.95, N 9.23. Found (%) : C 57.45, H 3.90, N 9.37. FT-IR (cm<sup>-1</sup>, KBr): 3057 (s), 1592 (s), 1575 (s), 663 (w), 420 (w). UV-Vis ( $\lambda$ , nm): 237, 279, 346, 363, 401, 639.

**Ni(L<sup>2</sup>)<sub>2</sub> (12):** Yield: 7.6 g (87%). Anal. Calcd. (%) for C<sub>42</sub>H<sub>34</sub>Br<sub>2</sub>N<sub>6</sub>O<sub>2</sub>Ni (*M*= 873.26): C 57.70, H 3.95, N 12.59. Found (%) : C 57.77, H 3.92, N 9.62. FT-IR (cm<sup>-1</sup>, KBr): 3035 (s), 1603 (s), 1594 (s), 512 (w), 417 (w). UV-Vis ( $\lambda$ , nm): 234, 292, 346, 394.

**Zn(4)<sub>2</sub> (14):** Yield: 3.7 g (82). Anal. Calcd. (%) for C<sub>26</sub>H<sub>20</sub>N<sub>2</sub>O<sub>2</sub>Zn (*M*= 457.83): C 68.21, H 4.40, N 6.12. Found (%) : C 67.97, H 4.42, N 6.62. FT-IR (cm<sup>-1</sup>, KBr): 3033 (s), 1603 (s), 1596 (s), 515 (w), 413 (w). UV-Vis ( $\lambda$ , nm): 234, 293, 341, 394.

### General procedure for the cycloaddition of epoxides to CO<sub>2</sub>

A 50 cm<sup>3</sup> stainless pressure reactor was charged with all of complexes (4.5·10<sup>-5</sup>mol), epoxide (4.5·10<sup>-2</sup>mol), and 4-dimethylaminopyridine (DMAP) (9·10<sup>-5</sup>mol). The reaction vessel was placed under a constant pressure of carbon dioxide for 2 min to allow the system to equilibrate and CO<sub>2</sub> was charged into the autoclave with desired pressure then heated to the desired temperature. The pressure was kept constant during the reaction. The vessel was then cooled to 5-10 °C in an ice bath after the expiration of the desired time of reaction. The pressure was released, then, the excess gases were vented. The yields of epoxides to corresponding cyclic carbonates were determined by GC (Agilent 7820A).

### Conclusions

In this study we have reported the synthesis and characterization of two novel ligands containing -N=N- group, and their metal complexes. In addition, a Zn complex of azo free form of L<sup>1</sup>H ligand **13** was prepared. The catalytic activity of the prepared metal complexes has been examined for the chemical fixation of CO<sub>2</sub> to corresponding cyclic carbonates with epoxides. Best

active catalyst has found to be Zn(L<sup>1</sup>)<sub>2</sub> **4** which was characterized by single crystal X-ray analysis. Different parameters have been investigated using this active complex as catalyst. From the comparison of all these complexes, azo group has positive effect to the catalytic activity. Catalytic studies are summarized as below:

- 1-Best active epoxide is found to be ECH,
- 2-Best active co-catalyst as base is found to be DMAP,
- 3-Best CO<sub>2</sub> atmosphere pressure is found to be 1.6 MPa,
- 4-125 °C is required for the catalytic conversion,
- 5-2 hours reaction time is enough for the coupling,
- 6-Ionic Liquid has been found to have a positive effect and showed the best active performance with (bmim)PF<sub>6</sub><sup>+</sup> Zn(L<sup>1</sup>)<sub>2</sub> as binary catalytic system.
- 7- Azo moiety increased the activity.

### Acknowledgements

The authors are grateful to TÜBİTAK (110T655) for research funds.

### Notes and references

- <sup>75</sup> <sup>a</sup>Department of Chemistry, Kahramanmaraş Sütçü İmam University, Kahramanmaraş, 46050-9, Turkey  
<sup>b</sup>Department of Chemistry, Harran University, Şanlıurfa, 63190, Turkey  
<sup>c</sup>Physics Department, Science and Arts Faculty, Kahramanmaraş Sütçü İmam University, 46100 Kahramanmaraş TURKEY.  
<sup>80</sup> <sup>d</sup>Science and Technology Application and Research Center, Dicle University, 21280 Diyarbakır TURKEY

\*Corresponding author: Tel.: +90(344)2801451, E-mail: esinispir@gmail.com. (E. İspir).

<sup>85</sup> † Electronic supplementary information (EIS) available: Crystal packing of the L<sup>1</sup>H ligand and its complex (Zn(L<sup>1</sup>)<sub>2</sub>), mass spectrum of L<sup>1</sup>H and L<sup>2</sup>H ligands, <sup>1</sup>H and <sup>13</sup>C-NMR spectrum of L<sup>1</sup>H and L<sup>2</sup>H ligands, Thermograms of complexes, experimental details have been deposited as supplementary material at the Cambridge Crystallographic Data Centre CCDC 1035285-1035286.

1. M. Ozdemir, *Inorg Chim Acta*, 2014, 421, 1-9.
2. S. K. Sarkar, M. S. Jana, T. Kumar Mondal and C. Sinha, *Appl Organomet Chem*, 2014, 28, 641-651.
3. A. G. F. Shoair, *J Coord Chem*, 2012, 65, 3511-3518.
4. A. Kilic, M. Ulusoy, M. Durgun, Z. Tasci, I. Yilmaz and B. Cetinkaya, *Appl Organomet Chem*, 2010, 24, 446-453.
5. M. A. Fuchs, C. Altesleben, T. A. Zevaco and E. Dinjus, *Eur J Inorg Chem*, 2013, 2013, 4541-4545.
6. S. Iksi, A. Aghmiz, R. Rivas, M. D. Gonzalez, L. Cuesta-Aluja, J. Castilla, A. Orejon, F. El Guemmout and A. M. Masdeu-Bulto, *J Mol Catal a-Chem*, 2014, 383, 143-152.
7. S. Liang, H. Liu, T. Jiang, J. Song, G. Yang and B. Han *Chem. Commun.*, 2011, 47, 2131-2133.
8. W. Cheng, X. Chen, J. Sun, J. Wang, S. Zhang *Catalysis Today*, 2013, 200, 117-124.
9. M. Ulusoy, A. Kilic, M. Durgun, Z. Tasci and B. Cetinkaya, *J Organomet Chem*, 2011, 696, 1372-1379.
10. K. Xu, J. G. Chen, Kuan-Wang, Z. W. Liu, J. Q. Jiang and Z. T. Liu, *J Macromol Sci A*, 2014, 51, 589-597.
11. C. Martín, G. Fiorani and A. W. Kleij, *ACS Catal.*, 2015, 5, 1353-1370.
12. S. Inoue, H. Koinuma and T. Tsuruta, *Journal of Polymer Science Part B: Polymer Letters*, 1969, 7, 287-292.
13. S. Kikuchi, S. Yoshida, Y. Sugawara, W. Yamada, H. M. Cheng, K. Fukui, K. Sekine, I. Iwakura, T. Ikeno and T. Yamada, *B Chem Soc Jpn*, 2011, 84, 698-717.
14. E. İspir, *Dyes Pigments*, 2009, 82, 13-19.

15. H. Atabey, E. Findik, H. Sari and M. Ceylan, *Turk J Chem*, 2014, 38, 109-120.
16. D. X. Huang, C. X. Wang and Y. B. Song, *Russ J Gen Chem+*, 2013, 83, 2361-2369.
17. S. Farhadi and S. Sepahvand, *J Mol Catal a-Chem*, 2010, 318, 75-84.
18. P. Govindaswamy, C. Sinha and M. R. Kollipara, *J Organomet Chem*, 2005, 690, 3465-3473.
19. M. Gulcan, S. Özdemir, A. Dündar, E. İspir and M. Kurtoğlu, *Zeitschrift für anorganische und allgemeine Chemie*, 2014, 640, 1754-1762.
20. Ş. Bitmez, K. Sayin, B. Avar, M. Köse, A. Kayraldız and M. Kurtoğlu, *J Mol Struct*, 2014, 1076, 213-226.
21. A.-N. M. A. Alaghaz, Y. A. Ammar, H. A. Bayoumi and S. A. Aldhlmani, *J Mol Struct*, 2014, 1074, 359-375.
22. E. Peker and S. Serin, *Synthesis and Reactivity in Inorganic and Metal-Organic Chemistry*, 2004, 34, 859-872.
23. K. Ouari, S. Bendia, J. Weiss and C. Bailly, *Spectrochim Acta A*, 2015, 135, 624-631.
24. H. A. Bayoumi, A.-N. M. Alaghaz and M. S. Aljahdali, *Int. J. Electrochem. Sci*, 2013, 8, 9399-9413.
25. M. Gaber, Y. S. El-Sayed, K. El-Baradie and R. M. Fahmy, *J Mol Struct*, 2013, 1032, 185-194.
26. E. İspir and S. Serin, *J Therm Anal Calorim*, 2008, 94, 281-288.
27. N. Karadayi, C. Albayrak, M. Odabasoglu and O. Buyukgungor, *Acta Crystallographica Section E*, 2006, 62, o1727-o1729.
28. W. Yang, X. L. You, Y. Zhong and D. C. Zhang, *Dyes Pigments*, 2007, 73, 317-321.
29. M. Aslantas, N. Kurtoglu, E. Sahin and M. Kurtoglu, *Acta Crystallographica Section E*, 2007, 63, o3637.
30. F. H. Allen, O. Kennard, D. G. Watson, L. Brammer, A. G. Orpen and R. Taylor, *J Chem Soc Perk T 2*, 1987, S1-S19.
31. H. Dal, Y. Suzen and E. Sahin, *Spectrochim Acta A*, 2007, 67, 808-814.
32. A. Kilic, M. V. Kilic, M. Ulusoy, M. Durgun, E. Aytar, M. Dagdevren and I. Yilmaz, *J Organomet Chem*, 2014, 767, 150-159.
33. A. Kilic, M. Ulusoy, M. Durgun and E. Aytar, *Inorg Chim Acta*, 2014, 411, 17-25.
34. A. Kilic, M. Ulusoy, M. Durgun, E. Aytar, A. Keles, M. Dagdevren and I. Yilmaz, *J Coord Chem*, 2014, 67, 2661-2679.
35. M. Ulusoy, E. Cetinkaya and B. Cetinkaya, *Appl Organomet Chem*, 2009, 23, 68-74.
36. Z. Tasci and M. Ulusoy, *J Organomet Chem*, 2012, 713, 104-111.
37. M. Ulusoy, O. Sahin, A. Kilic and O. Buyukgungor, *Catal Lett*, 2011, 141, 717-725.
38. G. M. Sheldrick, *University of Göttingen: Germany*, 1997.
39. G. M. Sheldrick, *University of Göttingen: Germany*, 1997.
40. L. Farrugia, *Journal of Applied Crystallography*, 1997, 30, 565.
41. J. Song, Z. Zhang, S. Hu, T. Wu, T. Jiang, B. Han, *Green Chem*, 2009, 11, 1031-1036.
42. D. J. Darensbourg, R. M. Mackiewicz, D. R. Billodeaux, *Organometallics*, 2005, 24, 144-148.
43. T. Lijima, T. Yamaguchi, *Appl Catal A: General*, 2008, 345, 12-17.
44. A. Kilic, M. Ulusoy, E. Aytar, M. Durgun, *Journal of Industrial and Engineering Chemistry*, 2015, 24, 98-106.
45. C. Jing-Xian, J. Bi, D. Wei-Li, D. Sen-Lin, C. Liu-Ren, C. Zong-Jie, L. Sheng-Lian, L. Xu-Biao, T. Xin-Man, A. Chak-Tong, *Appl Catal A: General*, 2014, 484, 26-32.
46. Y. Xie, Z. Zhang, T. Jiang, J. He, B. Han, T. Wu, K. Ding, *Angew Chem Int Ed*, 2007, 46, 7255-7258.
47. M. Nardelli, *Journal of Applied Crystallography*, 1995, 28, 659.
48. A. Spek, *Journal of Applied Crystallography*, 2003, 36, 7-13.
49. M. Odabasoglu, C. Albayrak, R. Ozkanca, F. Z. Aykan and P. Lonecke, *J Mol Struct*, 2007, 840, 71-89.
50. W. Rehman, F. Saman, I. Ahmad, *Russian Journal of Coordination Chemistry*, 2008, 34, 678-682.